BARBER, TERESA, S. M.S. The Study of Allosteric Modulator Sites at the cannabinoid CB1 Receptor. (2009)
Directed by Dr. Patricia Reggio. 57pp.

Org 27569, Org 27759 and Org 29647 are the first discovered allosteric modulators of the cannabinoid CB_1 receptor. These ligands are thought to bind to "accessory binding sites" at the receptor. Binding of the Org allosteric modulators has been shown to affect the affinities of various CB1 ligands, but to reduce the efficacy of these ligands. The goal of this research project was to understand at a molecular level, the origins of the effects produced by the Org allosteric modulators.

The study was begun by performing AM1 conformational searches for each allosteric modulator using the Spartan molecular modeling suite. Those conformers within 2.00 kcal/mol of the global minimum energy conformer of each modulator were subjected to geometry optimization in Jaguar (Schrodinger, Inc). Org27569 was then targeted for further study. Org 27569 has been reported to increase the CB1 affinity of the non-classical cannabinoid, (1R3R4R)-3-[2-hydroxy-4-(1,1-dimethylheptylphenyl]-4-(3-hydroxy-propyl)cyclohexab-1-ol, CP-55,940, but to reduce its efficacy.

Since the binding site of Org27569 is unknown, the MMC program was then employed to identify potential binding sites. The MMC program is a cavity biased method that uses Monte Carlo simulated annealing of chemical potential to identify small-molecule binding sites in protein structures via a molecular fragment approach [F. Guarnieri and M. Mezei,JACS 118, 8493, **1996**]. The receptor was placed in a virtual cell. At high chemical potentials, the box is filled with completely with the fragment of

interest. As the chemical potential decreases, fragments with less favorable interactions are stripped away. Indole and piperidine rings were used as fragments because they constitute the two major structural features of Org 27569. Three common binding sites for both the indole and piperidine fragments were identified. These areas were R3.50 (intracellular domain), W4.50 (possible homodimer interface) and in the transmembrane region between helices 1 and 2 (interacting with CP55,940). These were considered possible interaction sites for the following reasons: (1) If interactions occurred between the allosteric modulator and R3.50, this would block the interaction site of the G-protein and thus impair signalling. (2) W4.50 is commonly found in GPCR dimer interfaces. If the CB1 receptor functions as a dimer, Org27569 would impair activation by blocking dimer formation. (3) The TMH1-2 site site would allow the affinity of CP55940 to increase because it would block CP55940 exit from CB1. At the same time, the TMH1-2 site dock would constrain TMH6 from moving during activation by tethering the EC-3 loop. This should also result in impaired signal transduction. Future studies will involve mutation studies of each allosteric binding site identified in this project to determine the allosteric binding site for Org 27569.

THE STUDY OF ALLOSTERIC MODULATOR SITES

AT THE CANNABINOID CB1 RECEPTOR

By

Teresa S. Barber

A Thesis Submitted to
the Faculty of The Graduate School at
The University of North Carolina at Greensboro
in Partial Fulfillment
of the Requirements for the Degree
Master of Science

Greensboro
2009

Approved by

_____
Committee Chair

APPROVAL PAGE

This thesis has been approved by the following committee of the Faculty of the Graduate School at the University of North Carolina at Greensboro

Committee Chair _____

Committee Members _____

_____

_____
Date of Acceptance by Committee

_____
Date of Final Oral Examination

TABLE OF CONTENTS

Page

LIST OF TABLES

Page

LIST OF FIGURES

Page

CHAPTER I

INTRODUCTION TO G-PROTEIN COUPLED RECEPTORS AND THE CANNABINOID 1 RECEPTOR

The goal of this thesis project is to understand the action of novel allosteric modulators at the cannabinoid CB1 receptor. L.A Matsuda and co-workers first cloned and expressed the complimentary DNA that encoded the cannabinoid CB1 receptor from a rat cerebral cortex cDNA library in 1990 (Matsuda et al., 1990). The amino acid sequence of CB1 was found to be consistent with the tertiary structure of a G-protein coupled receptor (GPCR). Subsequently, the primary amino acid sequence of an N-terminus variant of CB1 and the sequences for human and mouse CB1 were reported (Abood et al., 1997; Gerard et al., 1991). The CB1 receptor is typically found in the central nervous system, however mRNA of CB1 has been identified in testis (Gerard et al.,1991).

. G-Protein Coupled Receptor Structure

G-protein coupled receptors (GPCRs) are a large group of proteins that are responsible for signal transduction. The structures of GPCRs include seven transmembrane alpha helices (TMHs) connected by intervening loops with an extracellular N-terminus and an intracellular C-terminus. In higher organisms, these receptors are responsible for the recognition of environmental stimuli. Some of these stimuli include light, taste, and odor. GPCRs are also responsible for other types of

communication across the plasma membrane. About 80% of all drug targets in the pharmaceutical industry today are GPCRs (Mirzadegan et al., 2003).

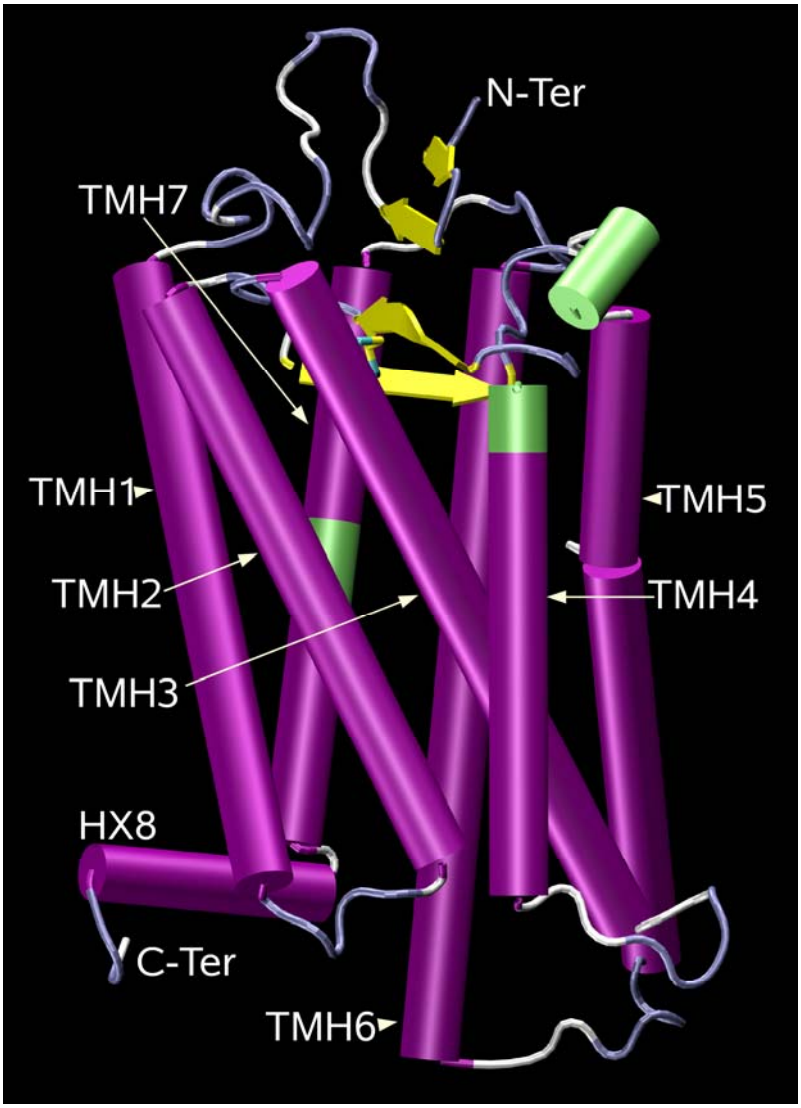

Figure 1: Generalized Structure of a G-Protein Coupled Receptor

One of the most commonly studied GPCRs is the dim light photoreceptor, rhodopsin. Rhodopsin is a member of the Class A GPCR family. This class comprises approximately ninety percent of all known GPCRs. Rhodopsin is activated by light and turns on a signaling pathway that leads to night vision. Rhodopsin is composed of a protein, opsin, to which a derivative of vitamin A , 11-*cis*-retinal , is covalently bound. Isomerization of 11-*cis*-retinal to all *trans*-retinal is initiated by absorption of a photon.

This isomerization leads to a conformational change in the protein that is the beginning of signal transduction (Palczewski et al., 2000).

The first x-ray crystal structure of bovine rhodopsin (in the dark (inactive) state) was reported by Palczewski and co-workers (Palczewski et al., 2000). In this structure (PDB #1F88), a total of 338 amino acid residues corresponding to 97.1% of the opsin molecule were resolved in the crystal structure. The last 15 residues of the C-terminus had to be modeled as alanines. Also resolved in the structure was the 11-*cis*-retinal chromophore (covalently bound to Lys296), as well as two zinc ions, three mercury ions and several water molecules.

The crystal structure of rhodopsin is important because it can serve as a structural template for other GPCRs. This includes the assignment of secondary structure and the location of highly conserved residues. Rhodopsin represents an intermediate size GPCR of the family and can feature most of the essential parts of functional importance in G-protein activation. The length of the helices and the extracellular loops are expected to be about the same for most Class A family members.

GPCR Signalling

GPCRs can be thought to exist in at least two states, the inactive (R) state and the activated (R*) state. Often the structure of a new protein can be modeled based on a homology structure of a well studied protein. For Class A GPCRs, the rhodopsin crystal structure is typically used to model the R state. There are several ways to model the activated state of GPCRs. One way to get a model of the activated state would be to use molecular dynamics (MD) simulations starting with the agonist bound in the inactive

state. However, MD simulations performed on very high performance computing clusters today reach only microseconds. In contrast, the time that it takes for rhodopsin to light activate has been estimated to be milliseconds (Arnis et al., 1994), while it takes seconds for the β2-AR (beta-2-adrenergic receptor) to be activated by its diffusible ligand (Ghanouni et al., 2001). Because GPCR activation takes much longer than the typical MD simulation will allow, it isn't possible at the current time to perform these simulations to study agonist induced changes to the R state to generate the R* state without intervening in the process using steered molecular dynamics, see for example (Saam et al., 2002).

Another way to approach building a model of a GPCR activated state is to build a model based on the conformational changes that have been suggested to occur by biophysical studies. Through biophysical studies of rhodopsin and the β2 adrenergic receptor, it has been shown that during activation there are rigid domain motions and rotations of transmembrane helices 3 and 6 (TMH3 and TMH6) that occur. These rotations are counterclockwise when one looks at the receptor from an extracellular view point (Farrens et al., 1996; Gether et al., 1997; Ghanouni et al., 2001). In rhodopsin, TMH3 and TMH6 are constrained at the intracellular end by a E3.49(134)/R3.50(135)/E6.30(247) salt bridge that limits the ability for the cytoplasmic ends of TMH3 and TMH6 to move in the inactive state (Palczewski et al., 2000). This salt bridge acts as an "ionic lock" (Ballesteros et al., 2001; Visiers et al., 2002). During activation, P6.50 of the highly conserved TMH6 CWXP motif acts as a hinge allowing TMH6 to straighten, moving its intracellular end away from TMH3 and up toward the

lipid bilayer (Altenbach et al., 2008; Jensen et al., 2001). This movement produces a break in the E3.49(134)/R3.50(135)/E6.30(247) salt bridge.

Based on the above information, a model of the CB1 activated state has been built in the Reggio lab. This model has been tested through mutation(Kapur et al., 2007; McAllister et al., 2004), substituted cysteine accessibility (Guo et al., 2005) and covalent probe (Khanolkar et al., 2000) experiments and the information from these experiments has been used to refine the model.

GPCR activation is thought, not only to involve changes in the intracellular domains, but also to involve a molecular switch within the ligand binding pocket (Kobilka and Deupi, 2007). This switch is a non-covalent intramolecular interaction that exists within the ligand binding pocket in the basal state of a GPCR that must be disrupted to achieve an active state. A commonly proposed switch is the "rotamer toggle switch" which involves W6.48 on TMH6 (Kobilka and Deupi, 2007; McAllister et al., 2004; Shi et al., 2002). In the dark (inactive) state of rhodopsin, the beta-ionone ring of 11-cis-retinal is close to W6.48(265) of the CWXP motif on TMH6 and acts as a lynch pin, constraining W6.48 in a χ_1 = g+ conformation (Li et al., 2004; Okada et al., 2002; Palczewski et al., 2000). In the light activated state, the beta-ionone ring moves away from TMH6 and toward TMH4 where it resides close to A4.58(169) (Borhan et al., 2000). This movement releases the constraint on W6.48(265), making it possible for W6.48(265) to undergo a conformational change. Lin and Sakmar (Lin and Sakmar, 1996) reported that perturbations in the environment of W6.48(265) of rhodopsin occur during the conformational change concomitant with receptor activation. This suggests

that the conformation of W6.48(265) when rhodopsin is in its inactive / ground state (R; χ_1 = g+) changes during activation (i.e., W6.48(265) χ_1 g+ $\rightarrow$ trans) (Shi et al., 2002). The CB_1 receptor contains a microdomain of aromatic residues that face into the ligand binding pocket in the TM3-4-5-6 region, including F3.25(189), F3.36(200), W4.64(255), Y5.39(275), W5.43(279) and W6.48(356). Singh and co-workers used the biased Monte Carlo/simulated annealing technique of Conformational Memories combined with receptor modeling to suggest that the F3.36(200)/W6.48(356) interaction in CB_1 may act as a mimic of the 11-cis-retinal/W6.48 interaction in the rhodopsin dark state and may serve as the "toggle switch" for CB_1 activation, with F3.36(200) χ1 *trans* / W6.48(356) χ1 *g+* representing the inactive (R) and F3.36(200) χ1 *g+* /W6.48(356) χ1 *trans* representing the active (R*) state of CB_1 (Singh et al., 2002). A detailed functional analysis of mouse CB_1 F3.36A and W6.48A mutants, undertaken to test this "toggle switch" hypothesis showed statistically significant increases in ligand-independent stimulation of GTPγS binding for a F3.36A mutant vs. WT mCB_1, while basal levels for the W6.48A mutant were not statistically different from WT mCB_1. These results suggested that F3.36 may function as a "linch pin", restraining W6.48 from moving to an active state conformation in the CB_1 receptor (McAllister et al., 2004). During activation of the CB1 receptor, the counterclockwise motion of TMH3 and TMH6 would cause F3.36 and W6.48 to move past each other. From an extracellular view point, one would see that W6.48 moves towards TMH5 and F3.36 moves towards TMH2.

While it has been common place to build models of GPCRs as monomers and some recent studies support monomeric GPCRs as functional units (Chabre and le Maire,

2005; Whorton et al., 2007), the emerging concept of GPCR dimerization has begun to challenge this notion. Recent work has shown not only that many GPCRs exist as homo- and heterodimers, but also that GPCR oligomeric assembly may have important functional roles. (Bulenger et al., 2005; Terrillon and Bouvier, 2004) At this point in the cannabinoid field, there is evidence of the functional importance of a CB1/ dopamine D2 heterodimer (Kearn et al., 2005; Reggio, 2006), but evidence for the functional significance of CB1 homodimers or oligomers has not been published. Therefore, in this thesis, only a monomeric CB1 model is considered.

CHART 1

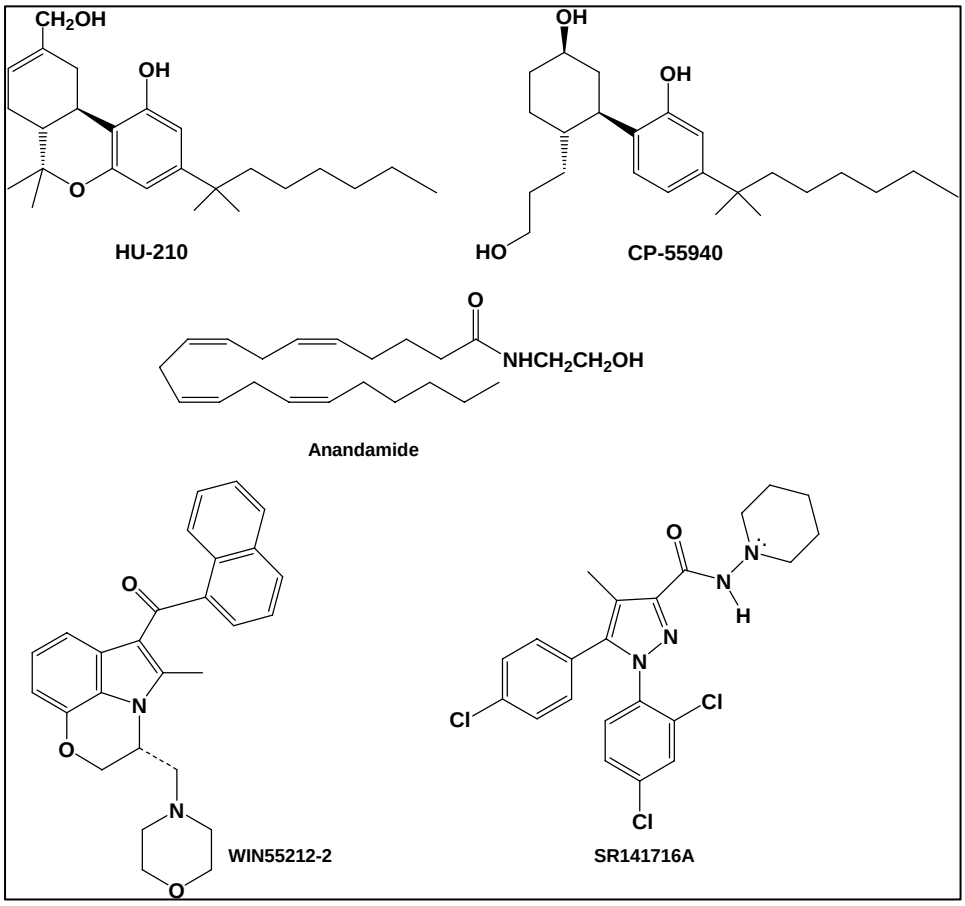

The CB1 receptor has five structurally distinct classes of ligands that can interact with it. The structures of these ligands are illustrated in Chart 1. Included in these are the classical cannabinoid agonists, such as (6aR)-trans-3-(1,1-dimethylheptyl)6a,7,10,10a-tetrahydro-1-hydroxy-6,6-dimethyl-6H-dibenzo[b,d]pyran-9-methanol), HU-210 ; non classical cannabinoid agonists, such as (1R3R4R)-3-[2-hydroxy-4-(1,1-dimethylheptylphenyl]-4-(3-hydroxy-propyl)cyclohexan-1-ol, CP-55,940; the endogenous cannabinoid agonists, such as, *N*-arachidonoylethanolamine, anandamide;

and, the aminoalkyindole (AA1) agonists such as 2,3-dihydro-5-methyl-3-[(4-morpholinyl)pyrrolo-[1,2,3-*de*]-1,4-benzoxazin-6-yl](1-naphyl)methanone, WIN55212-2. Diaryl pyrazole antagonist/inverse agonists such as *N*-(piperdin-1-yl)-5-(4-chlorophenyl)-1-(2,4-dichlorophenyl)-4-methyl-1*H*-pyrazole-3-carboxamide; SR141716A, have also been reported.

Both SR141716A and WIN55212-2 are highly aromatic compounds. Mutation studies have shown that each binds in the TMH3-4-5-6 region of CB1 (McAllister et al., 2003). However, these ligands favor different states of CB1. Because SR141716A is an inverse agonist, it will have higher affinity for the inactive (R) state. In the inactive state, SR141716A has been proposed to form aromatic stacking interactions with F3.36, Y5.39, and W5.43 (McAllister et al., 2004). SR141716A also forms a hydrogen bond with K3.28 (Hurst et al., 2002), a residue that is only available to the TMH3-4-5-6 region of CB1 in the inactive state. This hydrogen bond has been shown to be the key interaction which imparts the SR141716A preference for the R state (Hurst et al., 2006; Hurst et al., 2002). Figure 2 illustrates SR141716A docked in the CB1 R model. Residues with which SR has direct interactions are colored yellow, while residues that form part of the extended SR/CB1 complex are colored green.

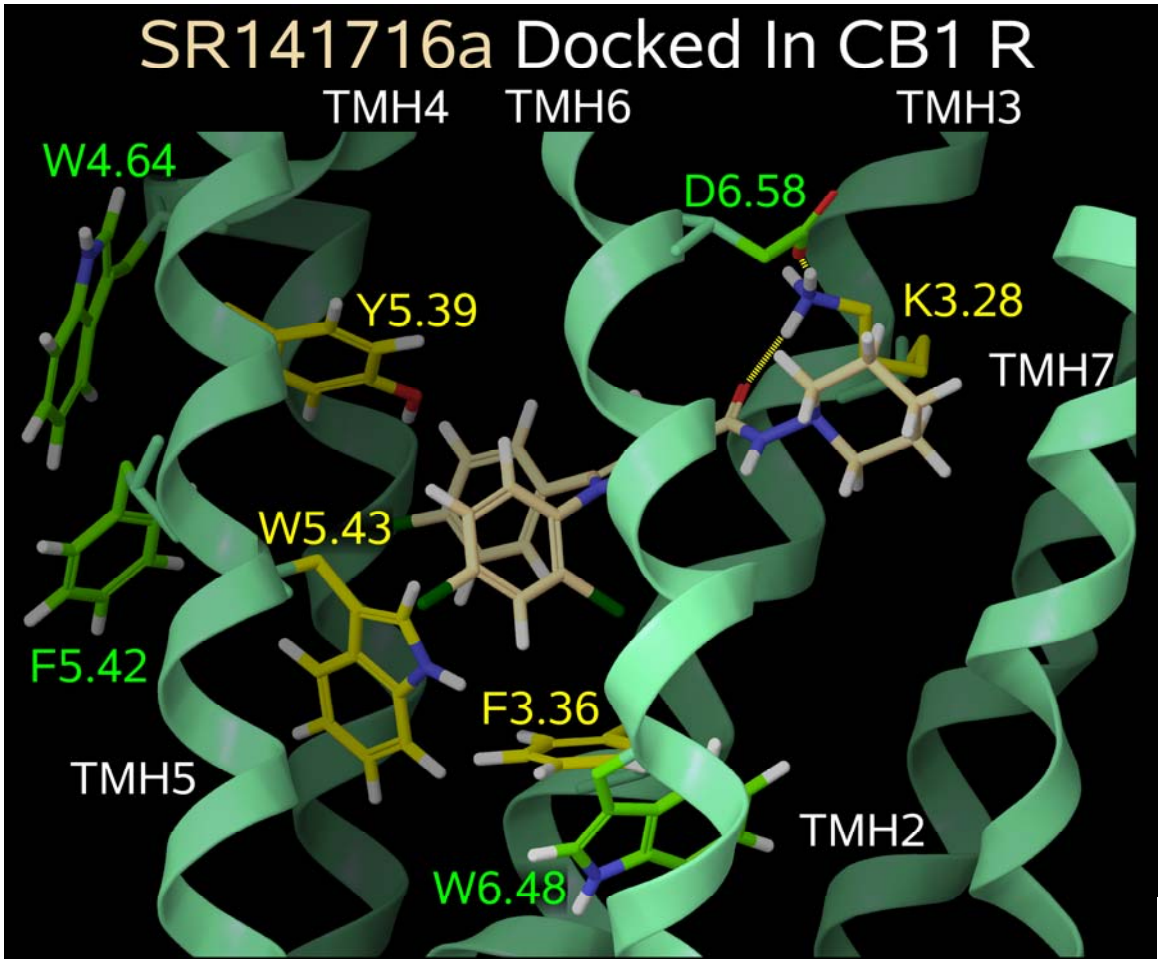

Figure 2: SR141716a Docked in the Inactive (R) State Model of the CB1 Receptor.

Because WIN55212-2 is an agonist, it will have higher affinity for the activated (R*) state. In the activated state, WIN 55-212-2 has been proposed to form interactions with F3.36, W5.43, and W6.48 (McAllister et al., 2004). In 1996, Song and Bonner (Song and Bonner, 1996) reported that mutation of K3.28 in CB1 to Ala resulted in a complete loss of HU210, CP55940 and anandamide (but not WIN55212-2) binding and a >100-fold decrease in EC_{50} for HU210, CP55940 and anandamide (but not WIN55212-2) upon this mutation. These results were confirmed later by Chin and co-workers (Chin et al., 1998). Figure 3 illustrates WIN55212-2 docked in the CB1 R* model. Residues with

which WIN has direct interactions are colored yellow, while residues that form part of the extended WIN/CB1 R* complex are colored green.

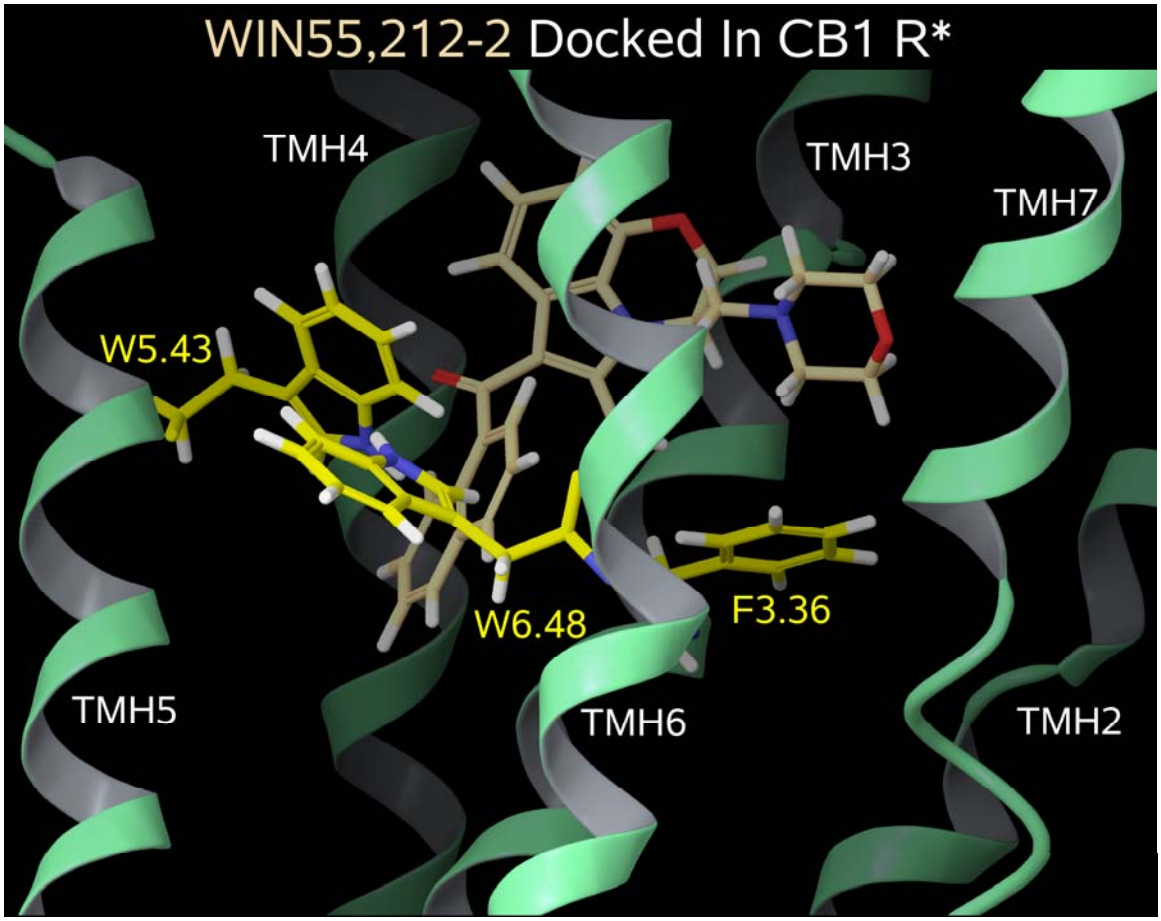

Figure 3: WIN55-212-2 Docked in the Activated (R*) State Model of the CB1 Receptor.

Mutation results reported by McAllister and co-workers have shown that the affinity of the cannabinoid agonist, CP55940 is unaffected by the F3.25A, F3.36A, W5.43A or W6.48A mutations (McAllister et al., 2003). These results suggest that unlike WIN55212-2, CP55940 does not bind in the TMH3-4-5-6 aromatic microdomain. Instead, modelling studies have suggested that CP55940 binds in the TMH2-3-6-7 region

of CB1 with a K3.28 hydrogen being the primary interaction site for CP55940 at CB1 and S1.39 and K(373) serving as secondary sites of interaction (see Figure 4). Kapur and co-workers (Kapur et al., 2007)recently reported that the CB_1 S7.39A mutant resulted in a total ablation of [^{3}H]CP55940 high affinity binding. This loss of binding was attributed to a change in TMH7 conformation upon this mutation that brings the extracellular end of TMH7 into the binding pocket of CP55940. Figure 4 illustrates CP55940 docked in the CB1 R* model. Residues with which CP has direct hydrogen bonding interactions are colored yellow.

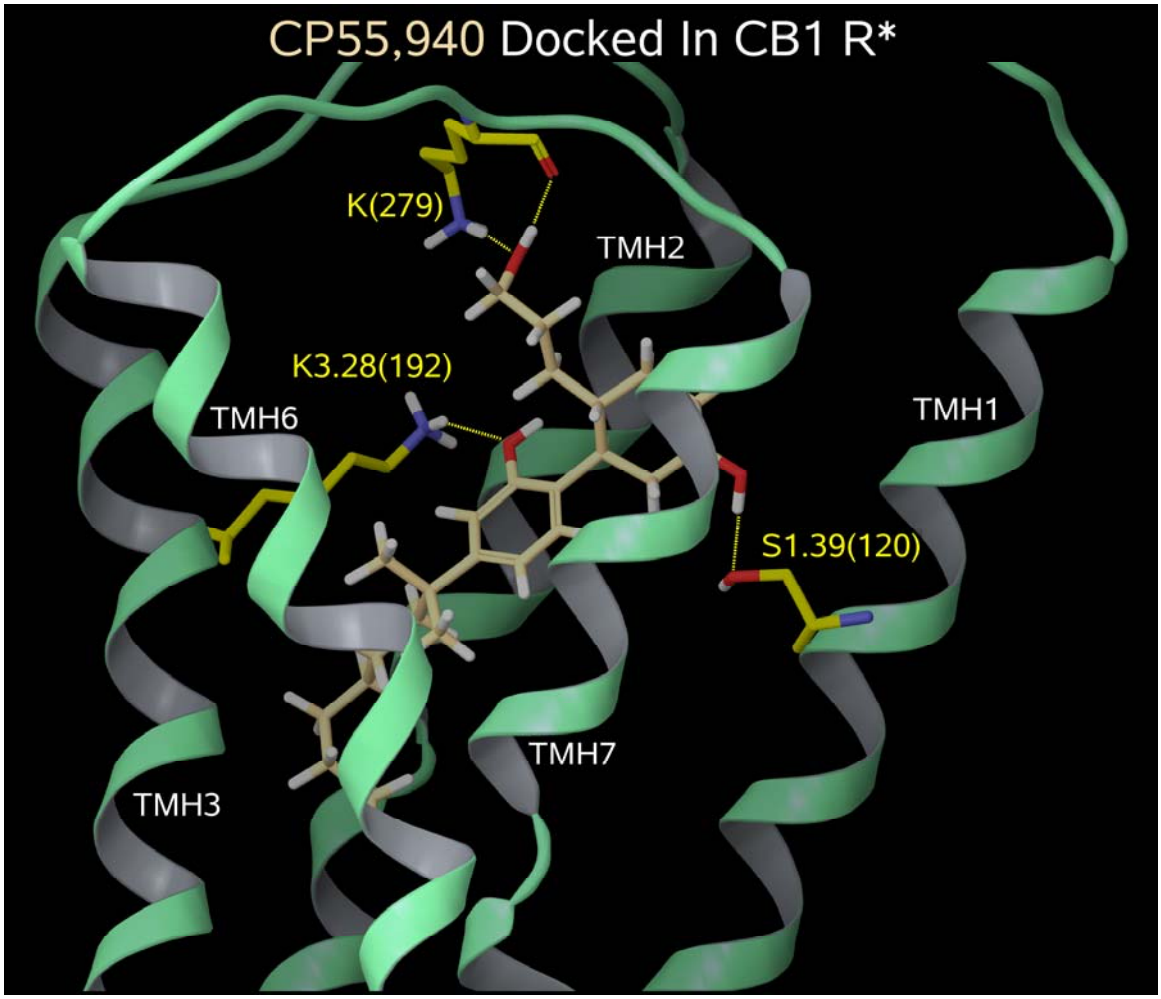

Figure 4: CP55,940 Docked in the Activated (R*) State Model of the CB1 Receptor.

CB_1 docking studies of the endogenous agonist anandamide in CB_1 R* have suggested that anandamide binds in a U shaped conformation in the TMH 2-3-6-7 region using K3.28 as its primary interaction site (McAllister et al., 2003). The binding site region identified for AEA by McAllister and co-workers has received support from modeling studies performed by Brizzi and co-workers (Brizzi et al., 2007). These authors found that AEA docks in the TMH2-3-6-7 region of CB_1 with the aliphatic chain directed toward the intracellular side of the receptor. The amide oxygen atom of AEA is hydrogen bonded to K3.28, while the hydroxyl group forms a hydrogen bond with S7.39. The n-pentyl tail of AEA is stabilized by lipophilic interactions with F3.25, V6.59, and F7.35 (Brizzi et al., 2007).

Allosteric Modulators

The binding site at which GPCR agonists bind and activate their receptors is termed the orthosteric site. Allosteric sites are "accessory binding sites" at which ligand binding can modulate (positively or negatively) the effect produced by the agonist at the orthosteric site. Allosteric modulators are characterized by the cooperativity factor, α, which quantifies the magnitude by which the affinity of one ligand is changed by the other ligand when both are bound to the receptor (i.e., the ratio of the binding constant of the allosteric site to that of the orthosteric site). The effect of allosteric modulators is saturable; i.e., once the allosteric sites are completely occupied, no further allosteric effect is observed. By contrast, classic orthosteric (competitive) antagonism can theoretically be infinite, as it depends only on the relative concentrations of the competing species. Saturability of allosteric effects applies to both positive and negative

allosteric modulators, and is therefore useful for drug candidates that are aimed at either enhancing or antagonizing receptor-mediated effects; the modulators can be given in relatively high doses without fear of overstimulating or overinhibiting the system (Christopoulos, 2002). Therefore, one reason for interest in allosteric modulators is that they can be prescribed with orthosteric compounds to minimize the dose of the orthosteric compound needed to achieve a desired pharmacological effect (Christopoulos and Kenakin, 2002).

Allosteric modulation can offer "absolute subtype selectivity". An example of this is the documented allosteric modulation produced by *N*-chloromethylbrucine at the muscarinic receptors when acetylcholine is the orthosteric ligand (see Table 1) (Christopoulos and Kenakin, 2002). $\text{Log}[K_A^{-1}]$ is a measure of the affinity of *N*-chloromethylbrucine for the receptor. Table 1 shows that while the affinities of *N*-chloromethylbrucine are in the same range, the cooperativity factors (α) are quite different. Here it is clear that *N*-chloromethylbrucine is only positively cooperative with acetylcholine at the M3 receptor (Christopoulos and Kenakin, 2002).

Table 1: Cooperative Factors with Acetylcholine at the M3 Receptor

Subtype	$Log[K_A^{-1}]$	α
M_1	4.38	0.45
M_2	4.22	0.094
M_3	3.66	3.26
M_4	4.32	1.03
M_5	3.66	0.055

Allosteric Modulators of the CB1 Receptor

Price and co-workers (Price et al., 2005) have shown that Org 27569 (5-Chloro-3-ethyl-1*H*-indole-2-carboxylic acid [2-(4-piperidin-1-yl-phenyl)-ethyl]-amide), Org 27759 (3-ethyl-5-fluoro-1*H*-indole-2-carboxylic acid [2-(94-dimethylamino-phenyl)-ethyl]-amide and Org 29647 (5-chloro-3-ethyl-1*H*-indole-2-carboxylic acid (1-benzyl-pyrrolidin-3-yl)-amide, 2-enedioic acid salt) are unexpectedly, allosteric enhancers of CB1 agonist binding affinity, but are functionally allosteric inhibitors of CB1 agonist signalling efficacy (see Figures 5 and 6). Horswill and co-workers(Horswill et al., 2007) recently reported a strikingly similar profile for PSNCBAM-1 (see Figure 7) (Horswill et al., 2007).

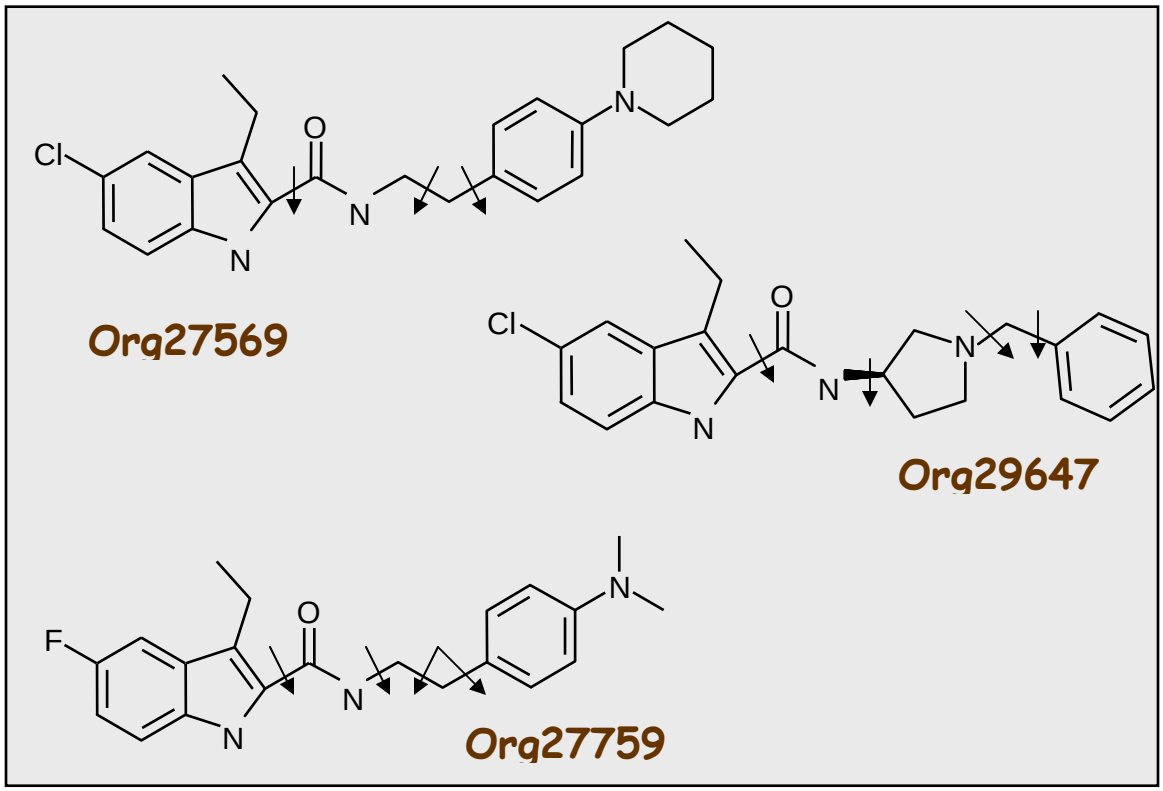

Figure 5: Allosteric Modulators for the CB1 Receptor. The arrows indicate bonds rotated during conformational analyses.

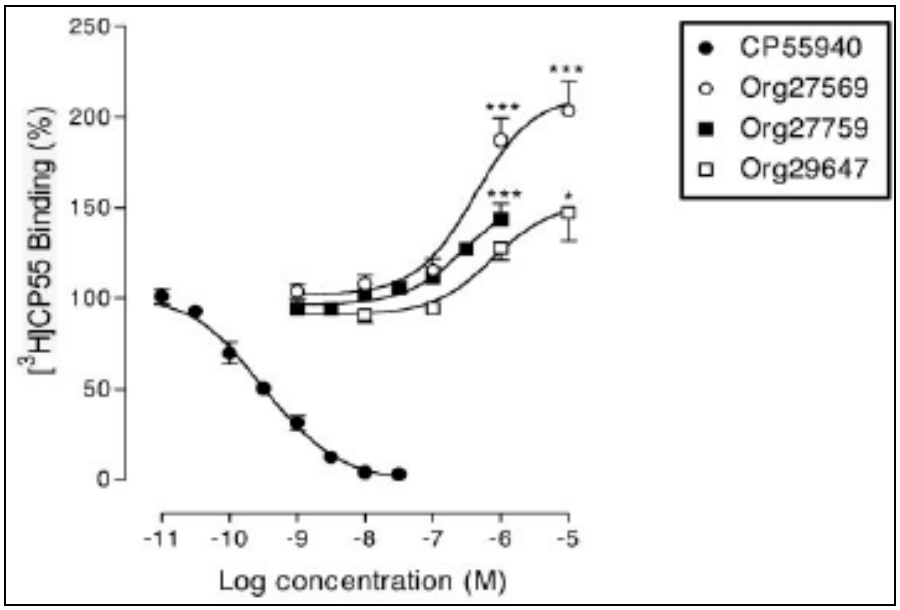

Figure 6: Binding Affinity Data for CP55,940 in the Presence of the Allosteric Modulators.

Figure 6 shows that in the presence of the Org allosteric modulators, ORG 27569 has the greatest affect on the binding of CP 55,940. While, Figure 8 shows that in the presence of ORG 27569, the signalling of CP55940 decreases dramatically (Price et al., 2005).

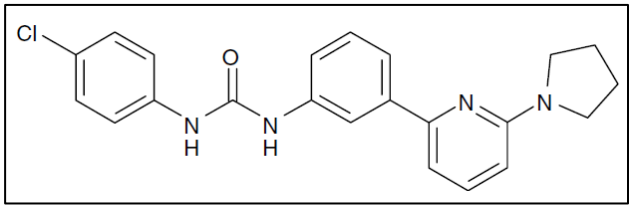

Figure 7: PSNCBAM-1

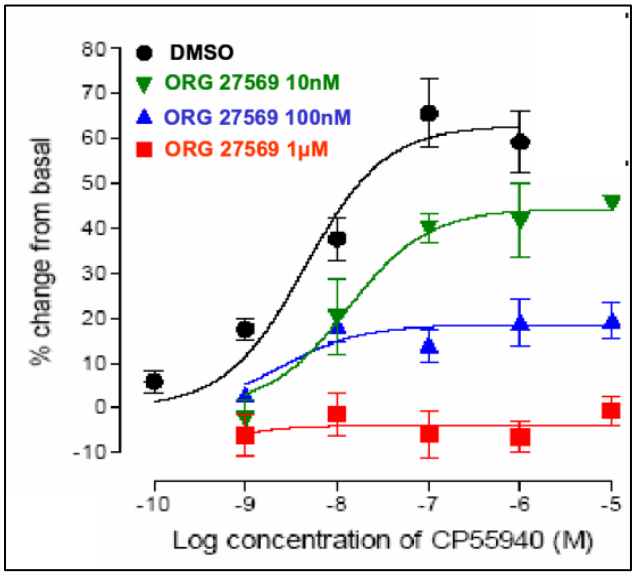

Figure 8: [^{35}S]GTPγS Binding in Mouse Brain Membranes in the Presence of ORG27569.

Taken together, Figures 6 and 8 show that the Org compounds display a ligand-dependent effect, whereby they enhance the specific binding of the CB_1 receptor agonist CP55940 but diminish its signalling. *Thus these ligands are allosteric enhancers of agonist binding affinity and allosteric inhibitors of agonist signalling efficacy.* The Org compounds are neither agonists nor antagonists in CB_1 receptor assay systems ([^{35}S]GTPγS binding in brain membranes, mouse isolated vas deferens and a CB_1 cAMP reporter assay), as they have no effect in the absence of agonist (Price et al., 2005).

The goal of this thesis project is to understand at the molecular level, the origins of the effects (presented in Figures 6 and 8) that are produced by Org27569, Org27759 and Org29647 on the binding of agonist, CP55940.

CHAPTER II

RESEARCH METHODS

Conformational Analysis

In order to understand the effects produced by Org27569, Org27759 and Org29647 on the binding of agonist, CP55940 at a molecular level, one first needs to understand the structure and flexibility of these compounds. To this end, the structure of each allosteric modulator was built in Spartan (Wavefunction INC, Irvin CA). A semi-empirical AM1 conformational analysis was performed on each allosteric modulator. Rotations were performed about each of the bonds marked by arrows in Figure 5. Once the conformational search was completed, each compound was examined and the global minimum energy conformation was identified. Minimum energy conformers that were within 2.00 kcal/mol of the global minimum were considered accessible conformations and were exported into Jaguar (Schrodinger New York, NY).

Jaguar Optimization

The conformation of the global minimum energy conformer and each minimum energy accessible conformer identified with AM1 was refined using a Hartree-Fock ab-initio geometry optimization at the 3-21G* level as encoded in Jaguar (Schrodinger, NewYork, NY). Results indicated that these ligands have low energy folded and extended conformations (see Results section, Figure 9).

Minimization of CB1 R* with Orthosteric Ligand (CP55940)

The wild type CB1 R* bundle with CP55940 docked was prepared and minimized as described in Kapur et. al. 2007(Kapur et al., 2007) . This model includes the CB1 trans membrane helix bundle, all intra- and extracellular loops, the complete C-terminus and a truncated N-terminus. This ligand/receptor model was used for all calculations described below.

Identification of Allosteric Binding Sites Using Grand Canonical Monte Carlo Simulations

The binding sites of the Org compounds have not yet been identified. In order to get an initial indication of where these compounds may bind at CB1, we used a novel cavity-biased grand canonical Monte Carlo method (MMC) (Guarnieri and Mezei, 1996) to identify regions of CB1 at which specific molecular fragments of the Org compounds bind. The MMC method is best described by Clark and co-workers (Clark et al, 2006):

The goal of this method is to create a series of grand canonical ensembles of ligands of interest interacting with a protein in a large simulation cell using Monte Carlo sampling (Clark, Guarnieri et al. 2006). The ligands are positioned throughout the cell

and over the entire surface of the protein. The free energy is annealed and the output of the calculation is an ensemble of ligand positions at each energy level in the annealing schedule. Annealing is typically run at descending free energy levels with each new level starting from the last ensemble generated from the previous run. There are several textbooks that show the derivation of the thermodynamics of the grand canonical ensemble (Friedman, 1985). The MMC approach has been used widely in surface science (He and Seaton, 2003; Meredith and Johnston, 1999; Nagumo, 2003). There has been limited use of the approach in chemistry (Jayaram and Beveridge, 1991).

In the grand canonical ensemble, the system energy is generally defined as the excess chemical potential relative to the chemical potential of a reference state, μ-μ_{ideal} - (Clark, Guarnieri et al. 2006). The unitless property, *B*, is used instead of directly using the excess chemical potential to set the system energry. The relationship between *B* and the number of ligands in the system, *N*, is show in equation 1 (Adams, 1975).

$$B=(\mu-\mu_{ideal})/kT+\ln N \qquad (1)$$

B is related to the concentration of molecules in the system as shown in equation 2. In MMC, it is *B* that is annealed rather than the chemical potential. One of the key features of the grand canonical ensemble is that the number of molecules in the system is varied by attempts to insert or delete molecules until the system density equilibrates to that particular chemical potential. The probability of accepting the insertion or deletion of a molecule into a system and the transforming from state i to j in terms of *B* is given in the equation below.

$$P_{ij}/P_{ji} = [V \exp(B - (E_i - E_j)/kT]/N_j \qquad (2)$$

The relationship of *B* to the system concentration can be emphasized by factoring equation 2.

$$(P_{ij}/P_{ji}) = (V/N_j)\exp(B)\exp(-\Delta E/kT) \qquad (3)$$

For an ideal gas, ΔE is always zero. At *B*=0, the above equation will result in a concentration of one molecule per system volume V. The reference state for the above condition is set by multiplying V/N by a reference concentration to make *B* represent the energy with respect to the reference state.

In the grand canonical ensemble, the ligands of interest can rotate and translate as well as leave or enter the system. These moves are attempted randomly and the probability of accepting the moves is given by equations 4-6.

$$\alpha_{insert} = \min[1, \exp(-\Delta E/kT + B)\, V/(N+1)] \qquad (4)$$

$$\alpha_{delete} = \min[1, \exp(-\Delta E/kT - B)\, N/V] \qquad (5)$$

$$\alpha_{move} = \min[1, \exp(-\Delta E/kT)] \qquad (6)$$

In the above equations, the term ΔE represents the change in potential energy for the move that is attempted. The unitless chemical potential and the temperature in Kelvin are represented by *B* and T, respectively. Equation 4 gives the probability of accepting the insertion of a new ligand into the system. In order to create a favorable interaction, the change in energy should be negative. This would make the value of the exponent in equation 4 positive and the insertion is likely to be a favorable move and thus accepted. Equation 5 gives the probability of a particular ligand leaving the system. In this case, if the change in energy is positive, then the exponent would be negative. This would mean

that the removal is likely because the ligand has created an unfavorable interaction. Note that for insertion the number of ligands changes from N to N+1 while for deletion the number of ligands changes from N+1 to N. Equation 6 represents the probability of accepting the rotation or translation of a ligand without changing the number of ligands present in the system. Equation 6 may also be used to calculate the probability of accepting conformational changes to the ligand of interest.

By using one or more of the above methods, a new configuration can be generated. The way the method determines if a move is accepted is by computing the change of energy and comparing it to a number that is randomly generated with a uniform distribution between 0 and 1. If the probability computed above is greater than the random number that was generated, then the move is accepted.

The states of the system, collected as snapshots characterized by N, and E (the average energy per ligand molecule) is the key outcome of a grand canonical ensemble simulation. After equilibration, the resulting ensemble of ligands corresponds to the free energy represented by the given *B* value (Clark, Guarnieri et al. 2006)

The MMC method has been used successfully to identify potent and novel p38 kinase inhibitors (Moore, 2005) and to identify thermolysin and T4 lysozyme binding sites (Clark et al., 2006). As initial tests of the MMC method, studies were performed to identify binding sites for water in bovine pancreatic trypsin inhibitor (BPTI) (Wlodawer et al., 1984), a protein for which good crystal structure information is available. A simple comparative study of three crystal structures of BPTI (PDB Numbers-1BPI, 5PTI and

6PTI) was performed. Once it was clear that the method was running properly, the study of the Org compounds at CB1 was undertaken. The molecular fragments used in this method were fragments relevant to the structures of the Org compounds (indole and piperidine rings). MMC runs were undertaken with the CB1 R* model (Kapur et al., 2007) and each fragment separately. Both the exterior and the interior of the receptor were sampled. Sites were sought at which the fragment clusters were consistent with the molecular structure of each compound. Clusters with molecular fragment spacing consistent with folded conformations identified for each compound, as well as extended conformations of each compound were considered.

Docking

Preliminary results from our conformational analysis indicated that the Org ligands have low energy folded and extended conformations. Results from MMC calculations determined whether the folded and/or extended conformer of each compound would be used for docking studies. Each Org conformer was then docked at each site identified by MMC calculations on the CB1 R* bundle using Maestro (Schrodinger New York, NY). This CB1 R* bundle had CP55940 docked at the orthosteric site as previously established via mutation studies(Kapur et al., 2007; McAllister et al., 2003; Picone et al., 2005)

Minimization of Bundle with Allosteric Modulator

The energy of docked ORG 27569 allosteric modulator positions to the CP55940 WT CB1 R* complex was minimized using the OPLS 2005 force field in Macromodel 9.1 (Schrödinger Inc., Portland, OR). An 8.0-Å extended nonbonded cutoff (updated

every 10 steps), a 20.0-Å electrostatic cutoff, and a 4.0-Å hydrogen bond cutoff were used in the calculation. A generalized born/surface area continuum solvation model for water, or GBSA model, as implemented in Macromodel was used for docking positions shown in figures 14 and 16 of the allosteric modulator. In each minimization the CP55940 WT CB1 R* complex was treated as non-moving fixed atoms as implemented in Macromodel 9.1, while the allosteric modulator ORG 27569 was completely free to move. Conjugate gradient minimization was performed for each docking position until a final gradient of 0.01 kcal/(mol(A^2)) was reached.

Assessment of Pair-wise Interaction Energies

Pair-wise interaction energies were then calculated between ORG 27569 and receptor residues within 4.0 Å. After defining the atoms of ORG 27569 as one group (group 1) and the atoms corresponding to a residue that lines the binding site in the final ligand/CB1 R* complex as another group (group 2), Macromodel (version 9.1) was used to output the pair-wise interaction energy (coulombic and van der Waals) for a given pair of atoms. The pairs corresponding to group 1 (ligand) and group 2 (residue of interest) were then summed to yield the interaction energy between the ligand and that residue. See Table 3.

The energies of interaction were compared for the orthosteric ligand (CP55940) in the presence and absence of the allosteric modulator (Org27569) at each site identified by MMC calculations. Allosteric sites were sought that would yield results consistent with the experimental results presented in Figures 6 and 8 above.

CHAPTER III

PRELIMINARY RESULTS

AM1 Conformational Searches

The global minimum energy conformations of Org27569, Org27759 and Org29647 were found to be folded conformations. However, extended conformations at 1.26 kcal/mol, 1.88 kcal/mol and 5.70 kcal/mol above the global minima were identified for Org27569, Org27759 and Org29647, respectively. For Org27569 and Org27759, these extended conformations were low enough in energy to be considered accessible at biological temperature.

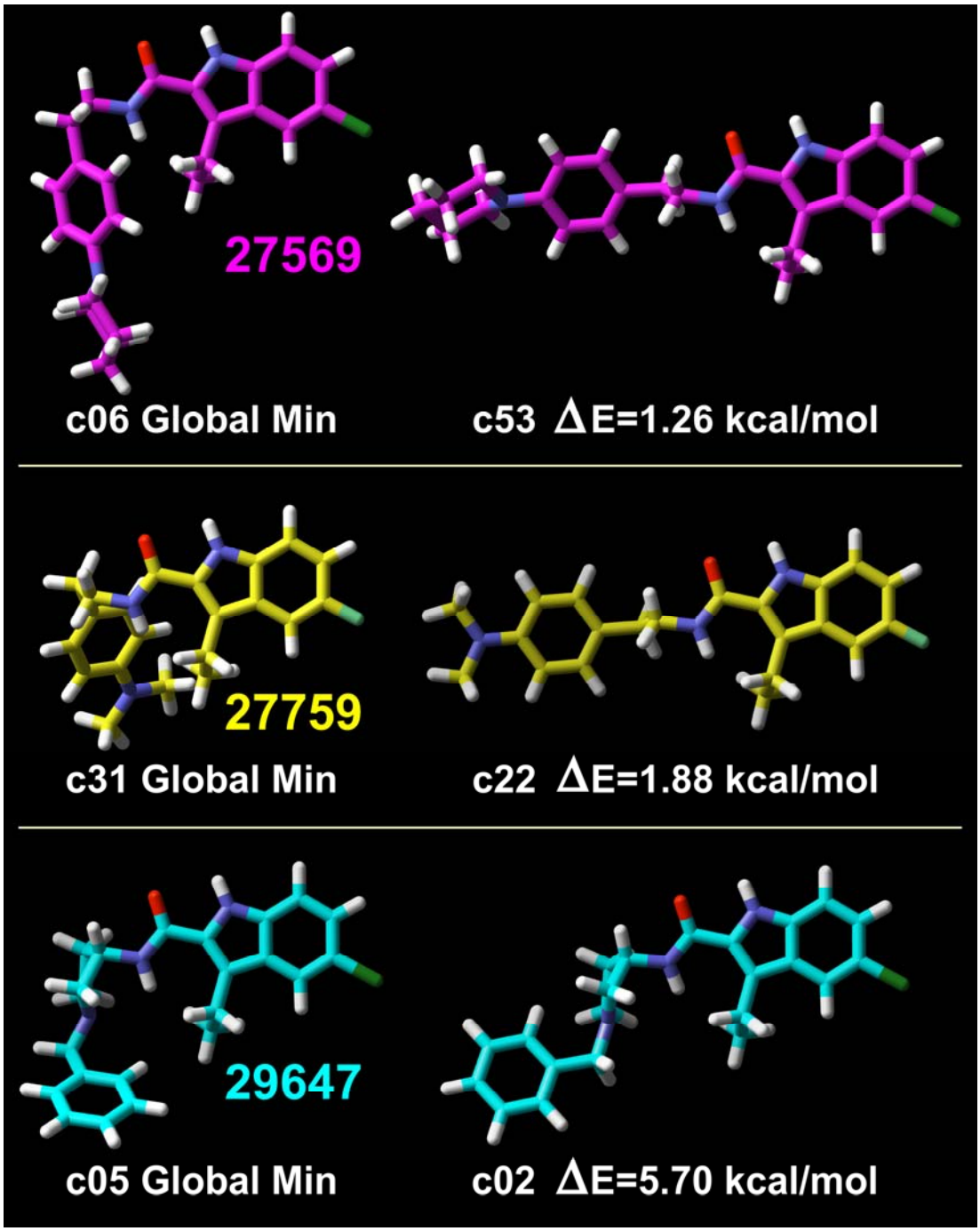

Figure 9: AM1 Conformational Search Results. The lowest energy folded and extended conformers of each Org compound are represented. In each case a folded conformation was the global minimum energy conformer.

Jaguar Optimization

Table 2 shows that the ab-initio optimization (performed in Jaguar) still identified the folded conformers to be the global minima. The relative energies of the extended conformers were very similar to those calculated using AM1.

Table 2: Ab-initio Relative Energies.

Org27569	Folded	Global min
	Extended	ΔE= +1.51 kcal/mol
Org27759	Folded	Global min
	Extended	ΔE=+1.75 kcal/mol
Org29647	Folded	Global min
	Extended	ΔE=+5.77 kcal/mol

. **Preliminary Docking Experiments**

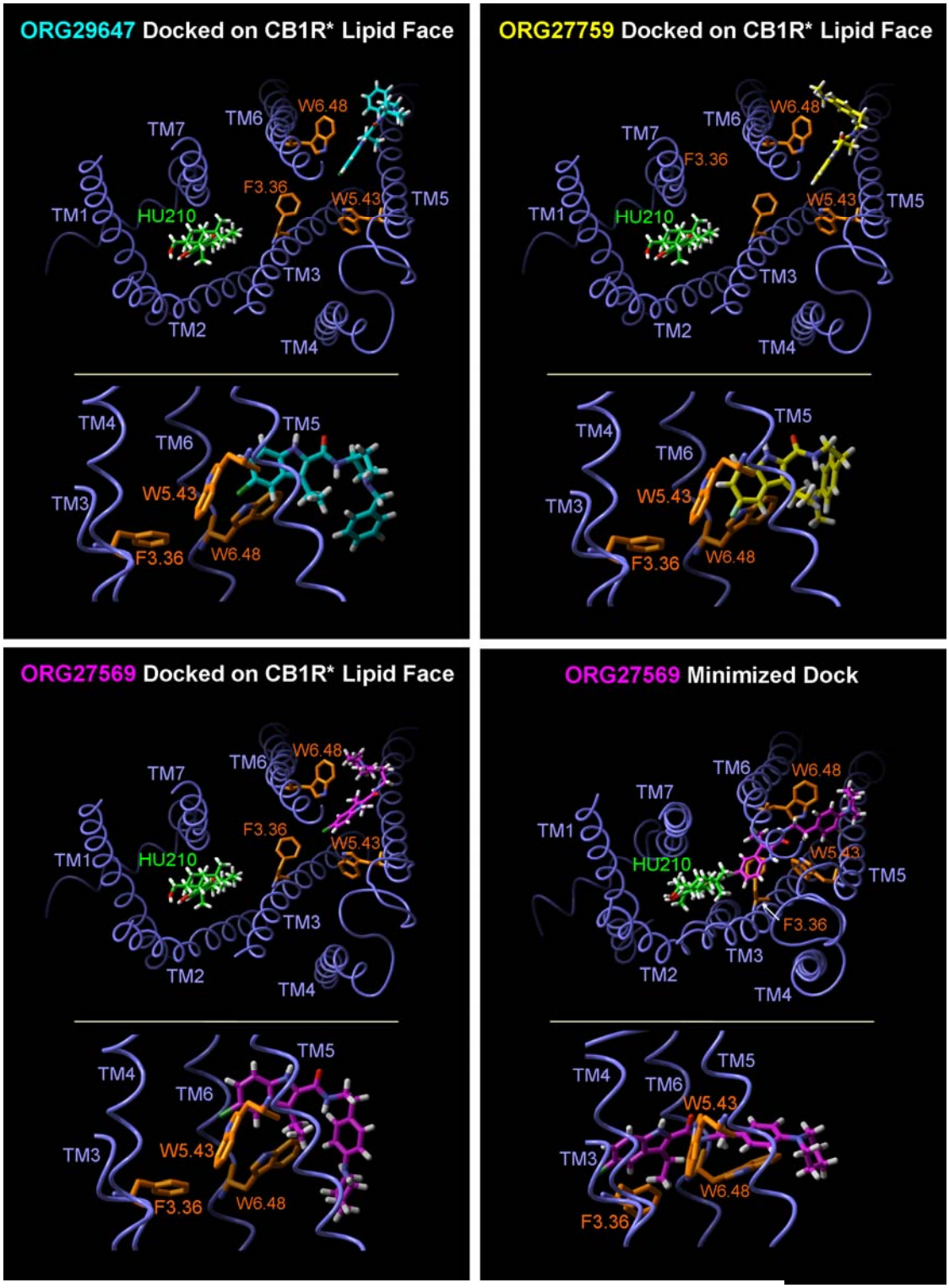

Figure 10: Preliminary Docks of all Three Org Allosteric Modulators.

Before beginning MMC calculations, an attempt was made to identify the allosteric sites for the Org compounds via hypothesis driven docking studies. The sites initially identified were based on the hypothesis that these compounds may bind at the interface of TMH5 and TMH6. In this location, many aromatic amino acids are available for interaction and the location would interfere with activation of the receptor. The results of initial docking studies were presented in Spring 2006 at the national ACS meeting in Atlanta. These sites are illustrated above in Figure 10. MMC studies were undertaken after these initial docking studies in order to identify alternate sites for each Org ligand.

MMC

As initial tests of the MMC method, studies were performed to identify binding sites for water in bovine pancreatic trypsin inhibitor (BPTI) (Wlodawer et al., 1984), a protein for which good crystal structure information is available. A simple comparative study of three crystal structures of BPTI: 1BPI, 5PTI and 6PTI was performed. After examining each of these crystal structures, four common/conserved internal waters and five common/conserved surface waters were identified. Three of the four internal waters form a triplet that hydrogen bonds to one another for stability. Conserved surface waters were found hydrogen bonding with residues R1, D3, T32, K46 and E49. Figure 11 illustrates results from the MMC study of BPTI. At left, the simulation cell containing BPTI and water at B = 10 is illustrated. Here water fills the simulation cell. At B = -7 (center), waters have been stripped away as the chemical potential is reduced. At B = -19

(right), only the bound waters identified in BPTI crystal structures remain, including the distinctive triplet waters.

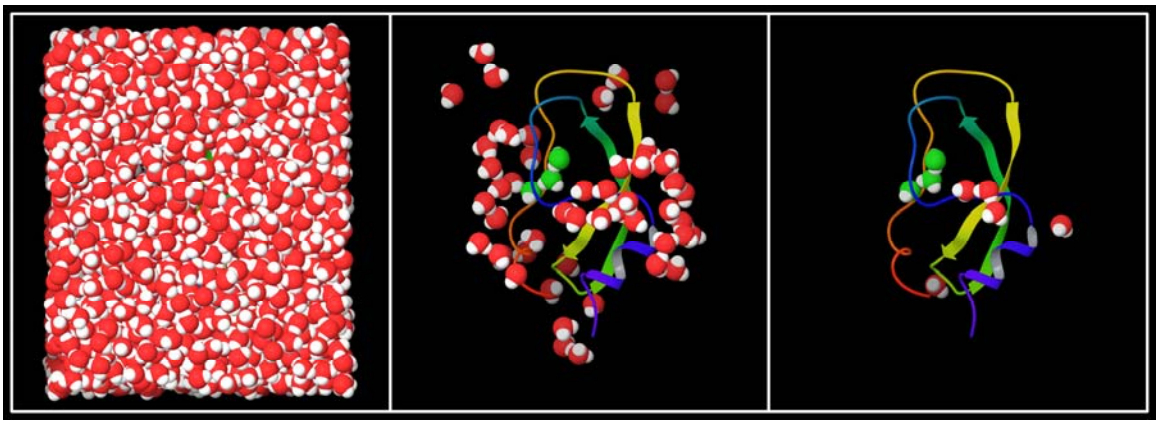

Figure 11: Initial MMC BPTI Runs. The initial MMC BPTI runs (Left, B= 10, Center B=-7; Right B=-19) are represented in the illustration. Waters are contoured at their Van der Waals radii. Internal waters are colored green, while external waters are colored red.

CHAPTER IV

RESULTS BASED OFF OF MMC STUDIES OF THE CB1 RECEPTOR

MMC Study of CB1

The MMC program was used to identify possible binding sites for indole and piperidine fragments (appropriate fragments of the Org structures) at the CB1 R*/CP55940 complex. Our goal was to identify sites at which not only ligand binding free energy was low, but also sites at which function would be impaired.

Figure 12 illustrates MMC results for the piperidine ring fragments at B= -2. Regions in which piperidine rings are colored yellow were those identified as plausible allosteric sites based upon their relationship with GPCR function. These three sites were (1) the region near R3.50, a key residue in the TMH3-6 intracellular salt bridge that is one toggle switch for GPCR activation; (2) W4.50, a residue commonly found in GPCR homodimer interfaces; and, (3) a TMH1-2 site near the orthosteric binding site.

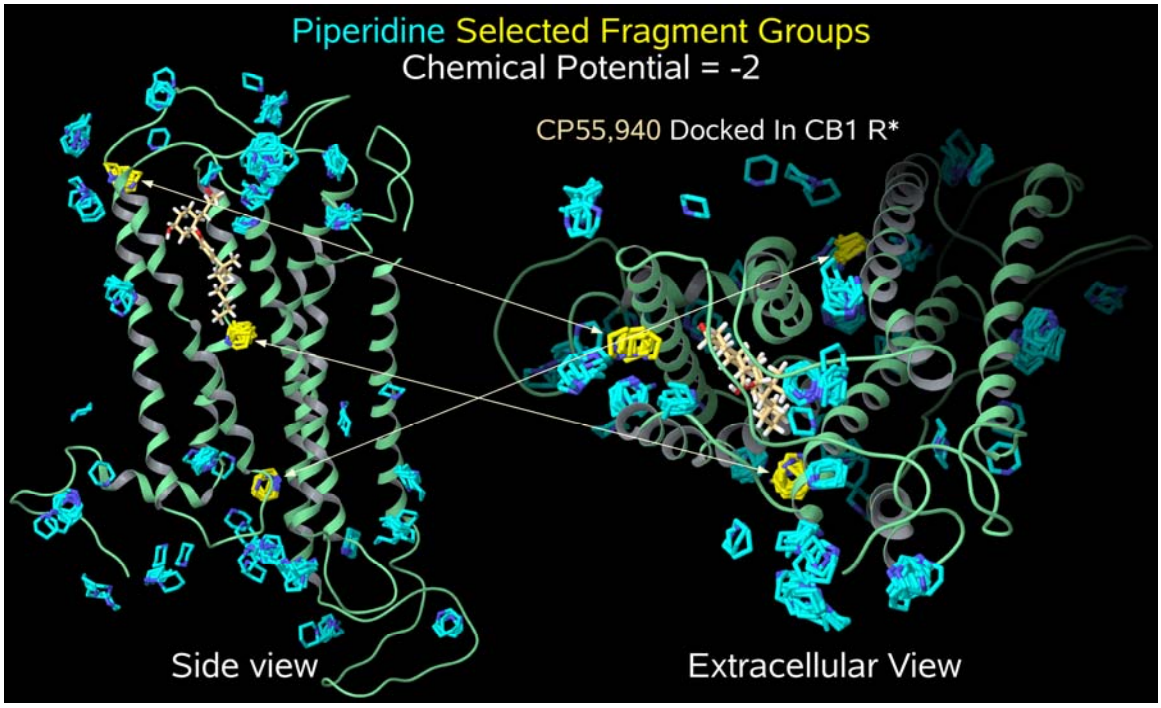

Figure 12: Original MMC Output of the Piperdine Fragment at B=-2 at the CB1 R*/CP55940 Complex. The yellow piperdines are those fragments that may represent possible binding sites of Org27569 consistent with its pharmacology.

Figure 13 illustrates MMC results for an indole fragment. At B= -5, there were many more indole fragments left compared with piperidine fragments above in Figure 12.

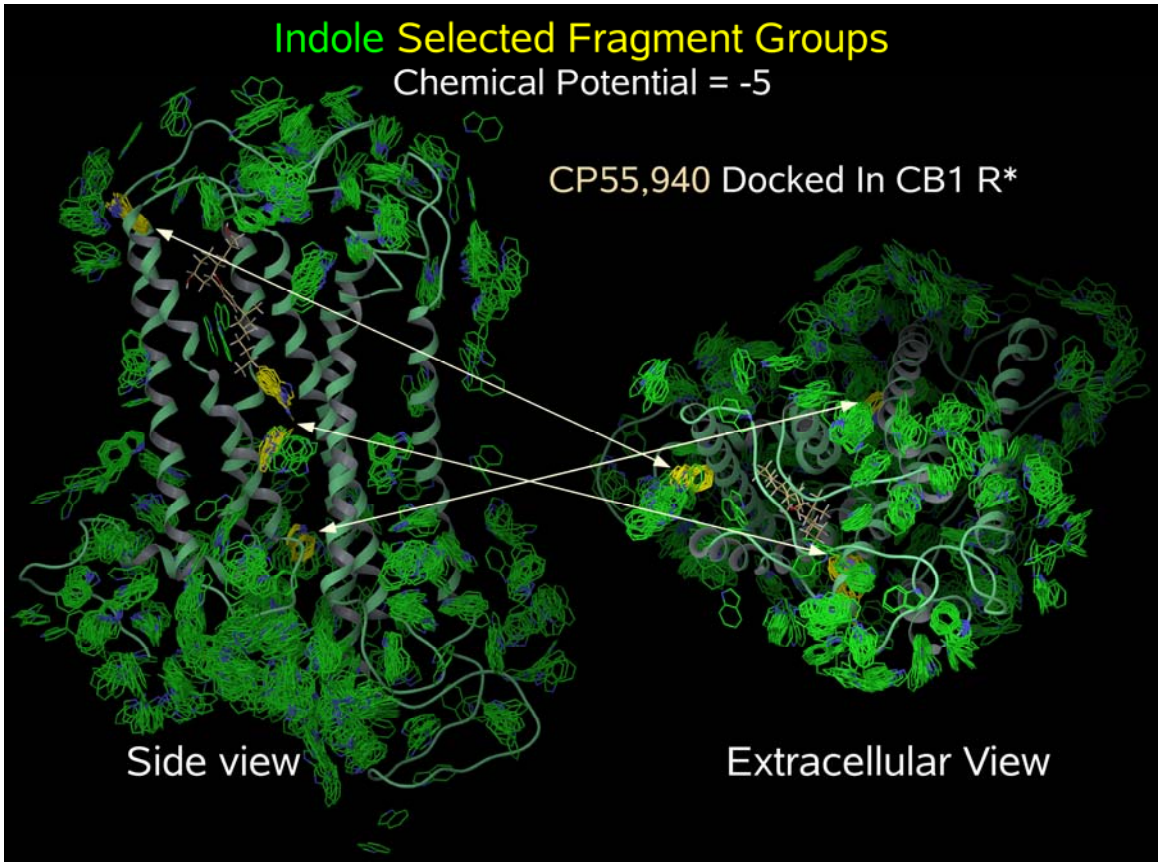

Figure 13: Original MMC Output of the Indole Fragment at B=-5 at the CB1 R*/CP55940 Complex. The yellow indoles are those fragments that correspond to regions identified with piperidine fragments in Figure 12.

These results were combined with the results of the piperdine runs in order to form hypotheses about where Org27569 could possibly dock. Notice that the piperdine fragments (Figure 12) cluster in three of the same places as the indoles (Figure 13) after their respective phase transitions. Based on the raw MMC results, three docking positions were hypothesized. These docks are illustrated in Figures 14-16 below.

(1) In Figure 14, Org27569 interacts with R3.50, a residue thought to stabilize the inactive state via a salt bridge with D6.30 (Ballesteros et al., 2001). This interaction is

broken in the activated state to open a crevice into which the G protein Gα C-terminus can dock. The interaction illustrated in Figure 14 would block interaction between the receptor and the G-protein and would therefore lead to impaired signaling. The fact that this interaction stabilizes the activated state of CB1, however, should lead to higher CP55940 affinity. It should be noted that this dock of Org27569 is plausible only if this compound can gain access to the intracellular domains of CB1.

(2) Barnett-Norris and co-workers (Barnett-Norris and Reggio, 2005) used Correlated mutation analysis (CMA) as implemented in the Filizola and Weinstein algorithim (Filizola and Weinstein, 2002) to identify TMH4 as the most likely homodimer interface for CB1. W4.50 is located in this dimer interface. Thus, if the Org compounds interact with W4.50 (as illustrated in Figure 15), they would interfere with dimerization. If the functional form of CB1 was a homodimer, allosteric modulator binding at W4.50 would, therefore, inhibit function, but again increase CP55940 affinity since the interaction stabilizes the activated state of CB1.

(3) In the dock shown in Figure 16, Org27569 interacts with CB1 near the extracellular ends of TMH1/2. This binding site would block exit of CP55940 from CB1 and thereby lead to an increase in the measured affinity of CP55940. The allosteric site identified here includes portions of the EC-3 loop (I(375)). Since TMH6 straightening is part of GPCR activation, this loop (which links TMH6 with TMH7) will also move upon

activation. It is concievable, then, that any interaction which tethers the IC-3 loop will lead to impaired signal transduction.

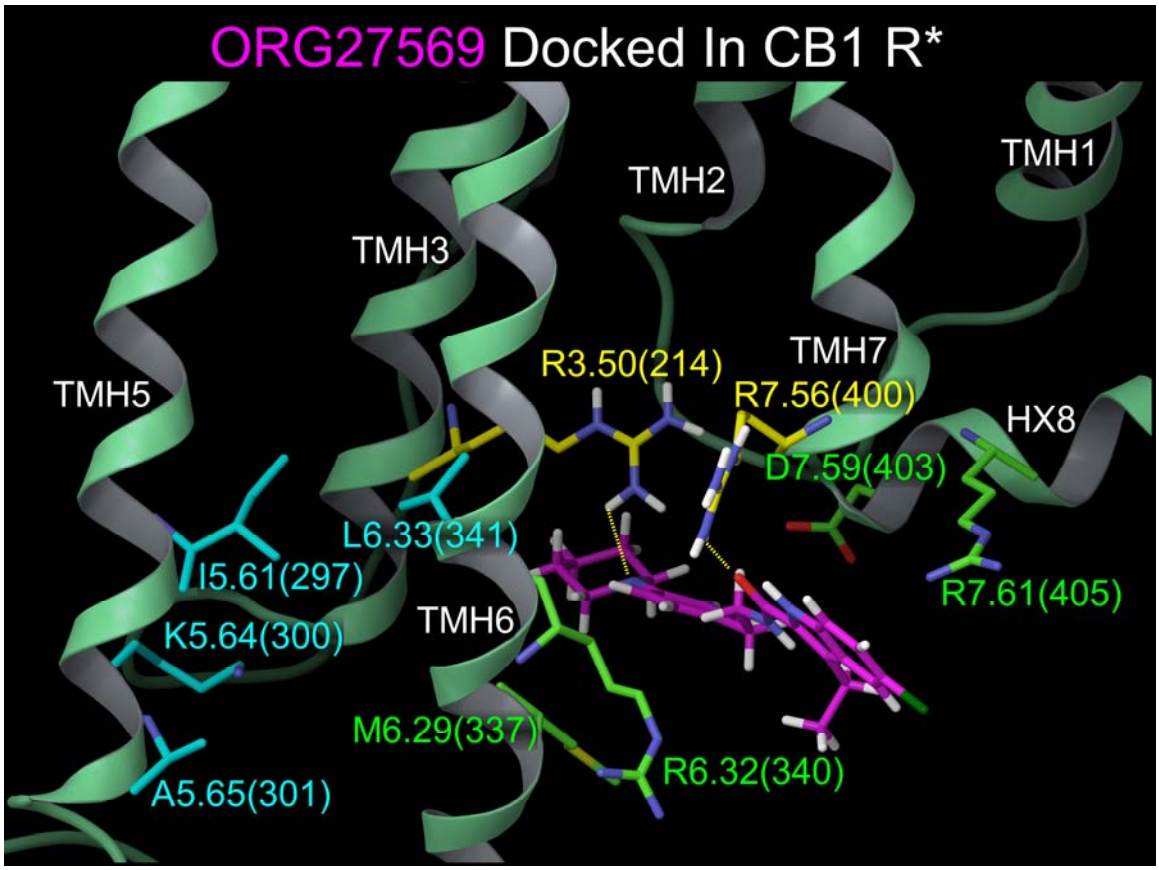

Figure 14: Org27569 Interacting with R3.50 and R7.56. The first allosteric modulator dock based on the MMC output. The total interaction energy for this dock is -33.2 kcal/mol. This interaction site would block interaction between the receptor and the G-protein and would therefore lead to impaired signaling.

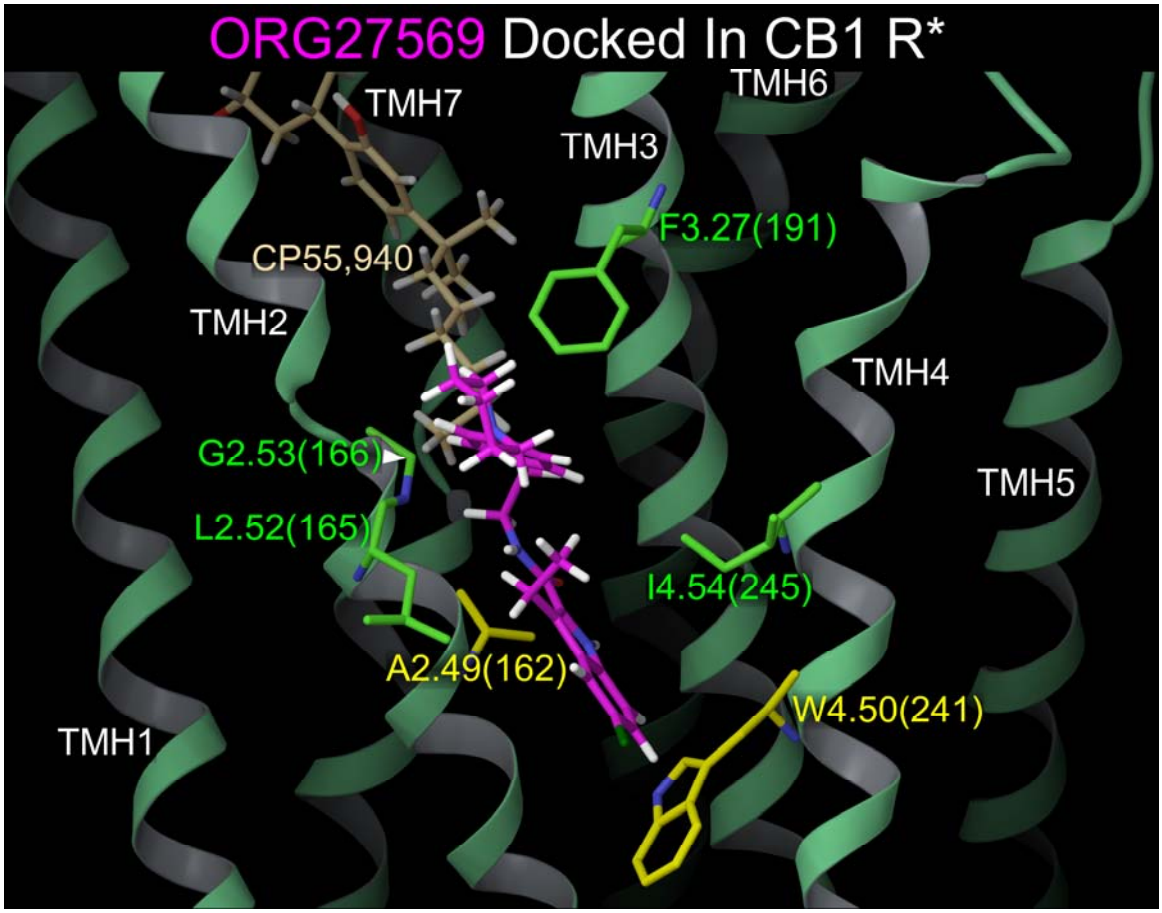

Figure 15: Org27569 Interacting with W4.50 and A2.49. The second allosteric modulator dock based on the MMC output. The total interaction energy for this dock is -16.3 kcal/mol. This would be a possible interaction site for Org 27569 if CB1 functions as a dimer, because the complex would block the TMH4 homodimer interface.

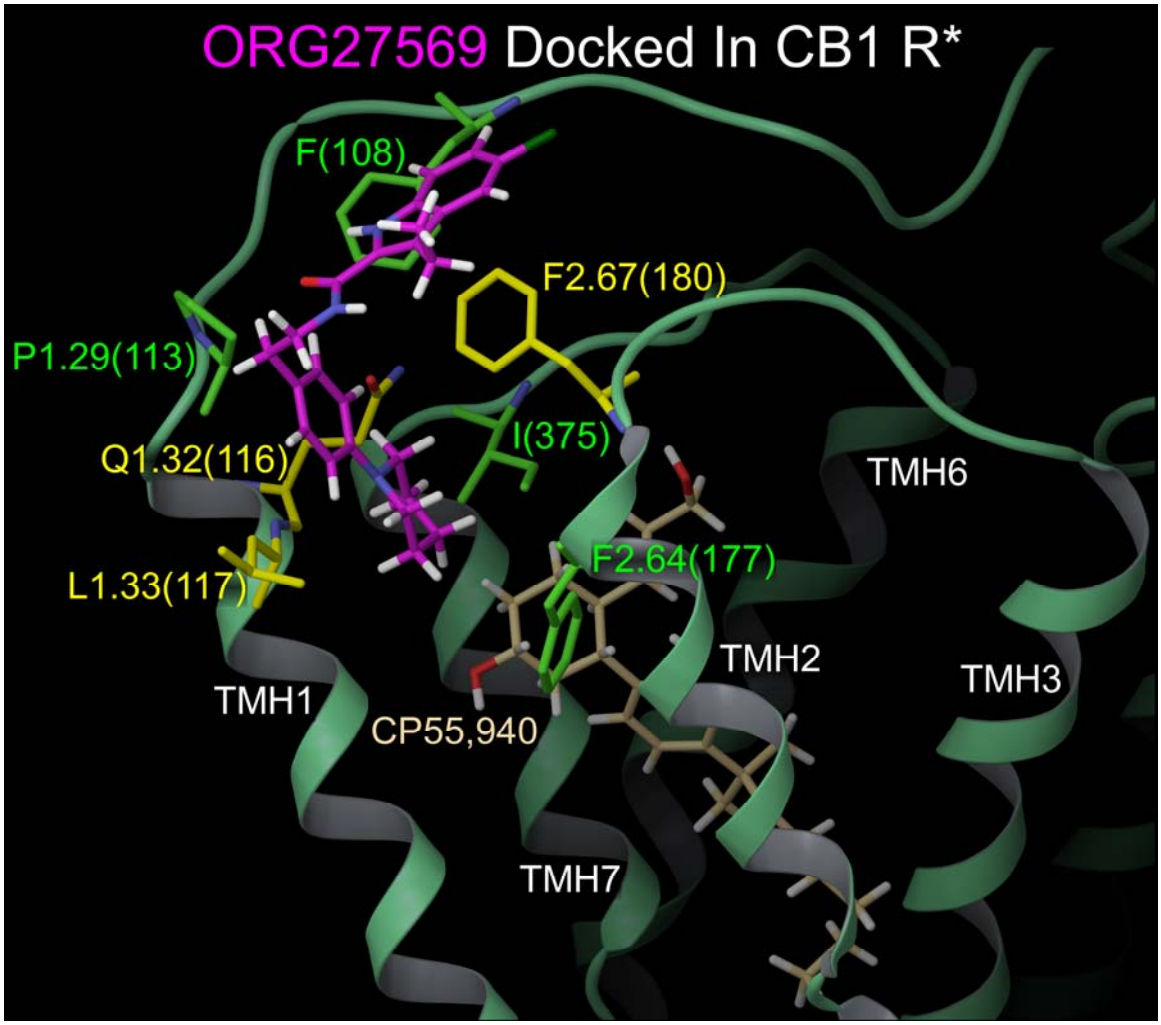

Figure 16: Org27569 Interacting with F2.67, Q1.32, and L1.33. The third allosteric modulator dock based on the MMC output. The total interaction energy for this dock is -24.2kcal/mol. This is a possibility because Org27569 would hold CB1 in a conformation that would allow the affinity of CP55940 to increase because it would block CP55940 exit from CB1. At the same time, this dock would constrain TMH6 from moving during activation by tethering the EC-3 loop. This should also result in impaired signal transduction.

Table 3: Energy Contributions for all Three Docks. Total energy includes Van der Waals and Coulomb interactions.

Dock R214	(Figure 14)	Dock TMH234	(Figure 15)	Dock TMH12	(Figure 16)
Residues	Total Energy (kcal/mol)	Residues	Total Energy (kcal/mol)	Residues	Total Energy (kcal/mol)
R214	-6.9	A162	-4.1	F108	-3.8
S217	-1.6	L165	-2.4	P113	-2.7
I218	-0.7	G166	-1.4	Q116	-3.6
R148	-0.8	V168	-0.3	L117	-4.0
M337	-3.4	I169	-0.3	A120	-1.3
R340	-3.3	F191	-2.3	F177	-2.8
R400	-11.3	W241	-3.4	F180	-4.6
K402	-2.4	I245	-2.1	H181	-0.5
R405	-2.8			I375	-0.9
Overall Energy	-33.2	Overall Energy	-16.3	Overall Energy	-24.2

Based on energetic considerations alone, the Org27569/CB1 R* complex illustrated in Figure 14, in which Org27569 interacts with R3.50 and R7.56 would be predicted to be the most likely interaction site for Org27569. However, this particular dock requires that the compound cross the membrane to access an intracellular site. The LogP of ORG27569 is 5.25 (organic-chemistry.com). Thus, it is likely that Org27569 will partition into lipid readily and some small fraction of the sample should be able to

cross the membrane to reach the intracellular compartment. The dock pictured in Figure 15, would require that Org27569 access the interaction site from lipid. Given its Log P value, this would seem to be possible. The dock in Figure 16 would be more likely if Org27569 were "druglike", i.e. could tolerate being in water. To determine this, Lipinski's Rule of Five was used.

Lipinski's Rule of Five

There is one way to define drug likeness of potential drug candidates by using four cutoff parameters. The cutoff parameters are close to five or multiples of five. Christopher A. Lipinski noted that when a potential drug has more than one value above the following that permeability is poor.

1. There are more than 5 H-bond donors.
2. The molecular weight is over 500.
3. The LogP is over 5 (Log P is the ratio of concentration of potential drug candidate dissolved in octanol to concentration of potential drug candidate dissolved in water).
4. There are more than 10 H-bond acceptors.

Lipinski's Rule of Five states that in general, an orally active drug has no more than one violation of the above criteria.

.(http://www.acdlabs.com/products/phys_chem_lab/logp/ruleof5.html).

When examining ORG27569, the following was found:

1. ORG27569 has two H-bond donors.
2. The molecular weight of ORG27569 is 410.
3. The LogP of ORG27569 is 5.25 (organic-chemistry.com).
4. ORG27569 has four H-bond acceptors.

According to Lipinski's rule of five, Org27569 should be orally active because it doesn't have more than one violation (log P is only violation) of the above rule.

Further Studies

Now that a hypothesis has been formed about the allosteric binding site, it will be necessary to undertake mutation studies to determine which of these hypothesized sites is more plausible. These studies are currently underway in Dr. Ruth Ross' laboratory at the University of Aberdeen in Scottland.

REFERENCES

Abood ME, Ditto KE, Noel MA, Showalter VM and Tao Q (1997) Isolation and expression of a mouse CB1 cannabinoid receptor gene. Comparison of binding properties with those of native CB1 receptors in mouse brain and N18TG2 neuroblastoma cells. *Biochem Pharmacol* **53**(2):207-214.

Adams D (1975) Grand Canonical Ensemble Monte Carlo for a Lennard Jones Fluid. *J Mol Phys* **29**:307-311.

Altenbach C, Kusnetzow AK, Ernst OP, Hofmann KP and Hubbell WL (2008) High-resolution distance mapping in rhodopsin reveals the pattern of helix movement due to activation. *Proc Natl Acad Sci U S A* **105**(21):7439-7444.

Arnis S, Fahmy K, Hofmann KP and Sakmar TP (1994) A conserved carboxylic acid group mediates light-dependent proton uptake and signaling by rhodopsin. *J Biol Chem* **269**(39):23879-23881.

Ballesteros JA, Jensen AD, Liapakis G, Rasmussen SG, Shi L, Gether U and Javitch JA (2001) Activation of the beta 2-adrenergic receptor involves disruption of an ionic lock between the cytoplasmic ends of transmembrane segments 3 and 6. *J Biol Chem* **276**(31):29171-29177.

Barnett-Norris J and Reggio PH (2005) Identification of Possible CB1/Dopamine D2 Heterodimer Interfaces Using Correlated Mutation Analysis, in *2005 Symposium on the Cannabinoids* (Musty R ed), ICRS, Clearwater, Florida.

Borhan B, Souto ML, Imai H, Shichida Y and Nakanishi K (2000) Movement of retinal along the visual transduction path. *Science* **288**(5474):2209-2212.

Brizzi A, Cascio MG, Brizzi V, Bisogno T, Dinatolo MT, Martinelli A, Tuccinardi T and Di Marzo V (2007) Design, synthesis, binding, and molecular modeling studies of new potent ligands of cannabinoid receptors. *Bioorg Med Chem* **15**(16):5406-5416.

Bulenger S, Marullo S and Bouvier M (2005) Emerging role of homo- and heterodimerization in G-protein-coupled receptor biosynthesis and maturation. *Trends Pharmacol Sci* **26**(3):131-137.

Chabre M and le Maire M (2005) Monomeric G-protein-coupled receptor as a functional unit.*Biochemistry***44**(27):9395-9403.

Chin C, Lucas-Lenard J, Abadji V and Kendall DA (1998) Ligand Binding and Modulation of Cyclic AMP Levels Depend on the Chemical Nature of Residue 192 of the Human Cannabinoid Receptor 1. *J Neurochem* **70**:366-373.

Christopoulos A (2002) Allosteric binding sites on cell-surface receptors: novel targets for drug discovery. *Nat Rev Drug Discov* **1**(3):198-210.

Christopoulos A and Kenakin T (2002) G protein-coupled receptor allosterism and complexing. *Pharmacol Rev* **54**(2):323-374.

Clark M, Guarnieri F, Shkurko I and Wiseman J (2006) Grand canonical Monte Carlo simulation of ligand-protein binding. *J Chem Inf Model* **46**(1):231-242.

Farrens DL, Altenbach C, Yang K, Hubbell WL and Khorana HG (1996) Requirement of Rigid-Body Motion of Transmembrane Helicies for Light-Activation of Rhodopsin. *Science* **274**:768-770.

Filizola M and Weinstein H (2002) Structural models for dimerization of G-protein coupled receptors: The opioid receptor homodimers. *Biopolymers* **66**(5):317-325.

Friedman HL (1985) *A Course in Statistical Thermodynamics*. Prentice Hall, Englewood Cliffs, NJ.

Gerard CM, Mollereau C, Vassart G and Parmentier M (1991) Molecular cloning of a human cannabinoid receptor which is also expressed in testis. *Biochem J* **279 (Pt 1)**:129-134.

Gether U, Lin S, Ghanouni P, Ballesteros JA, Weinstein H and Kobilka BK (1997) Agonists induce conformational changes in transmembrane domains III and VI of the beta2 adrenoceptor. *Embo J* **16**(22):6737-6747.

Ghanouni P, Steenhuis JJ, Farrens DL and Kobilka BK (2001) Agonist-induced conformational changes in the G-protein-coupling domain of the beta 2 adrenergic receptor. *Proc Natl Acad Sci U S A* **98**(11):5997-6002.

Guarnieri F and Mezei M (1996) Simulated annealing of chemical potential: A general procedure for locating bound waters. Application to the study of the differential hydration propensities of the major and minor grooves of DNA. *J Am Chem Soc* **118**:8493-8494.

Guo W, Shi L, Filizola M, Weinstein H and Javitch JA (2005) From The Cover: Crosstalk in G protein-coupled receptors: Changes at the transmembrane homodimer interface determine activation. *Proc Natl Acad Sci U S A* **102**(48):17495-17500.

He Y and Seaton NA (2003) Experimental and Computer Simulation Studies of the Adsorption of Ethane, Carbon Dioxide, and Their Binary Mixtures in MCM-41. *Langmuir* **19**:10132-10138.

Horswill JG, Bali U, Shaaban S, Keily JF, Jeevaratnam P, Babbs AJ, Reynet C and Wong Kai In P (2007) PSNCBAM-1, a novel allosteric antagonist at cannabinoid CB(1) receptors with hypophagic effects in rats. *Br J Pharmacol* **152**(5):805-814.

http://www.acdlabs.com/products/phys_chem_lab/logp/ruleof5.html.

Hurst D, Umejiego U, Lynch D, Seltzman H, Hyatt S, Roche M, McAllister S, Fleischer D, Kapur A, Abood M, Shi S, Jones J, Lewis D and Reggio P (2006) Biarylpyrazole inverse agonists at the cannabinoid CB1 receptor: importance of the C-3 carboxamide oxygen/lysine3.28(192) interaction. *J Med Chem* **49**(20):5969-5987.

Hurst DP, Lynch DL, Barnett-Norris J, Hyatt SM, Seltzman HH, Zhong M, Song ZH, Nie J, Lewis D and Reggio PH (2002) N-(piperidin-1-yl)-5-(4-chlorophenyl)-1-(2,4-dichlorophenyl)-4-methyl-1H-p yrazole-3-carboxamide (SR141716A) interaction with LYS 3.28(192) is crucial for its inverse agonism at the cannabinoid CB1 receptor. *Mol Pharmacol* **62**(6):1274-1287.

Jayaram B and Beveridge DL (1991) Grand canonical Monte Carlo simulations on aqueous solutions of sodium chloride and sodium DNA: excess chemical potentials and sources of nonideality in electrolyte and polyelectrolyte solutions. *J Phys Chem* **95**:2506-2516.

Jensen AD, Guarnieri F, Rasmussen SG, Asmar F, Ballesteros JA and Gether U (2001) Agonist-induced conformational changes at the cytoplasmic side of transmembrane segment 6 in the beta 2 adrenergic receptor mapped by site-selective fluorescent labeling. *J Biol Chem* **276**(12):9279-9290.

Kapur A, Hurst DP, Fleischer D, Whitnell R, Thakur GA, Makriyannis A, Reggio PH and Abood ME (2007) Mutation Studies of Ser7.39 and Ser2.60 in the Human CB1 Cannabinoid Receptor: Evidence for a Serine-Induced Bend in CB1 Transmembrane Helix 7. *Mol Pharmacol* **71**(6):1512-1524.

Kearn CS, Blake-Palmer K, Daniel E, Mackie K and Glass M (2005) Concurrent stimulation of cannabinoid CB1 and dopamine D2 receptors enhances heterodimer formation: a mechanism for receptor cross-talk? *Mol Pharmacol* **67**(5):1697-1704.

Khanolkar AD, Palmer SL and Makriyannis A (2000) Molecular probes for the cannabinoid receptors. *Chem Phys Lipids* **108**(1-2):37-52.

Kobilka BK and Deupi X (2007) Conformational complexity of G-protein-coupled receptors. *Trends Pharmacol Sci* **28** (8):397-406.

Li J, Edwards PC, Burghammer M, Villa C and Schertler GF (2004) Structure of bovine rhodopsin in a trigonal crystal form. *J Mol Biol* **343**(5):1409-1438.

Lin S and Sakmar T (1996) Specific tryptophan UV-absorbance changes are probes of the transition of rhodopsin to its active state. *Biochemistry* **35**(34):11149-11159.

Matsuda LA, Lolait SJ, Brownstein MJ, Young AC and Bonner TI (1990) Structure of a cannabinoid receptor and functional expression of the cloned cDNA. *Nature* **346**(6284):561-564.

McAllister SD, Hurst DP, Barnett-Norris J, Lynch D, Reggio PH and Abood ME (2004) Structural mimicry in class A G protein-coupled receptor rotamer toggle switches: the importance of the F3.36(201)/W6.48(357) interaction in cannabinoid CB1 receptor activation. *J Biol Chem* **279**(46):48024-48037.

McAllister SD, Rizvi G, Anavi-Goffer S, Hurst DP, Barnett-Norris J, Lynch DL, Reggio PH and Abood ME (2003) An Aromatic Microdomain at the Cannabinoid CB(1) Receptor Constitutes an Agonist/Inverse Agonist Binding Region. *J Med Chem* **46**(24):5139-5152.

Meredith JC and Johnston KP (1999) Density Dependence of Homopolymer Adsorption and Colloidal Interaction Forces in a Supercritical Solvent: Monte Carlo Simulation. *Langmuir* **15**:8037-8044.

Mirzadegan T, Benko G, Filipek S and Palczewski K (2003) Sequence analyses of G-protein-coupled receptors: similarities to rhodopsin. *Biochemistry* **42**(10):2759-2767.

Moore WR (2005) Maximizing discovery efficiency with a computationally driven fragment approach. *Curr Opin Drug Disc Devel* **8**(3):355-364.

Nagumo RT, H.; Nakao, S (2003) S.-I. Prediction of Ideal Permeability of Hydrocarbons through an MFI-Type Zeolite Membrane by a Combined Method Using Molecular Simulation Techniques and Permeation Theory. *J Phys Chem* **B**(107):14422-14428.

Okada T, Fujiyoshi Y, Silow M, Navarro J, Landau EM and Shichida Y (2002) Functional role of internal water molecules in rhodopsin revealed by X-ray crystallography. *Proc Natl Acad Sci U S A* **99**(9):5982-5987.
organic-chemistry.com.

Palczewski K, Kumasaka T, Hori T, Behnke CA, Motoshima H, Fox BA, Le Trong I, Teller DC, Okada T, Stenkamp RE, Yamamoto M and Miyano M (2000) Crystal structure of rhodopsin: A G protein-coupled receptor. *Science* **289**(5480):739-745.

Picone RP, Khanolkar AD, Xu W, Ayotte LA, Thakur GA, Hurst DP, Abood ME, Reggio PH, Fournier DJ and Makriyannis A (2005) (-)-7'-Isothiocyanato-11-hydroxy-1',1'-dimethylheptylhexahydrocannabinol (AM841), a high-affinity electrophilic ligand, interacts covalently with a cysteine in helix six and activates the CB1 cannabinoid receptor. *Mol Pharmacol* **68**(6):1623-1635.

Price MR, Baillie GL, Thomas A, Stevenson LA, Easson M, Goodwin R, McLean A, McIntosh L, Goodwin G, Walker G, Westwood P, Marrs J, Thomson F, Cowley P, Christopoulos A, Pertwee RG and Ross RA (2005) Allosteric modulation of the cannabinoid CB1 receptor. *Mol Pharmacol* **68**(5):1484-1495.

Reggio PH (2006) Computational methods in drug design: modeling G protein-coupled receptor monomers, dimers, and oligomers. *Aaps J* **8**(2):E322-336.

Saam J, Tajkhorshid E, Hayashi S and Schulten K (2002) Molecular dynamics investigation of primary photoinduced events in the activation of rhodopsin. *Biophys J* **83**(6):3097-3112.

Shi L, Liapakis G, Xu R, Guarnieri F, Ballesteros JA and Javitch JA (2002) Beta 2 adrenergic receptor activation. Modulation of the proline kink in transmembrane 6 by a rotamer toggle switch. *J Biol Chem* **277**(43):40989-40996.

Singh R, Hurst DP, Barnett-Norris J, Lynch DL, Reggio PH and Guarnieri F (2002) Activation of the cannabinoid CB1 receptor may involve a W6.48/F3.36 rotamer toggle switch. *J Pept Res* **60**(6):357-370.

Song ZH and Bonner TI (1996) A lysine residue of the cannabinoid receptor is critical for receptor recognition by several agonists but not WIN55212-2. *Mol Pharmacol* **49**(5):891-896.

Terrillon S and Bouvier M (2004) Roles of G-protein-coupled receptor dimerization. *EMBO Rep* **5**(1):30-34.

Visiers I, Ebersole BJ, Dracheva S, Ballesteros J, Sealfon SC and Weinstein H (2002) Structural motifs as functional microdomains in G-protein-coupled receptors: Energetic considerations in the mechanism of activation of the serotonin 5-HT2a receptor by disruption of the ionic lock of the arginine cage. *Int J Quantum Chem* **88**:65-75.

Whorton MR, Bokoch MP, Rasmussen SG, Huang B, Zare RN, Kobilka B and Sunahara RK (2007) A monomeric G protein-coupled receptor isolated in a high-density lipoprotein particle efficiently activates its G protein. *Proc Natl Acad Sci U S A* **104**(18):7682-7687.

Wlodawer A, Walter J, Huber R and Sjolin L (1984) Structure of bovine pancreatic trypsin inhibitor. Results of joint neutron and X-ray refinement of crystal form II. *J Mol Biol* **180**(2):301-329.